De novo origins of multicellularity in response to predation

Matthew D. Herron[1,2], Joshua M. Borin[2], Jacob C. Boswell[1,2], Jillian Walker[2], I-Chen Kimberly Chen[2], Charles A. Knox[1], Margrethe Boyd[1,3], Frank Rosenzweig[1,2], and William C. Ratcliff[2]

1. University of Montana, Division of Biological Sciences, Missoula, MT
2. Georgia Institute of Technology, School of Biological Sciences, Atlanta, GA
3. Northwestern University, Department of Biomedical Engineering, Evanston, IL

Corresponding author: Matthew D. Herron, xprinceps@gmail.com

Author contributions:

Conceived the project: MDH, FR, WCR

Carried out the experiments: MDH, JMB, JCB, JW, CAK, MB, WCR

Analyzed the data: MDH, JMB, JW, I-CC, CAK, WCR

Wrote the manuscript: MDH, JMB, JCB, I-CC, CAK, MB, FR, WCR

Summary

The transition from unicellular to multicellular life was one of a few major events in the history of life that created new opportunities for more complex biological systems to evolve. Predation is hypothesized as one selective pressure that may have driven the evolution of multicellularity. Here we show that *de novo* origins of simple multicellularity can evolve in response to predation. We subjected outcrossed populations of the unicellular green alga *Chlamydomonas reinhardtii* to selection by the filter-feeding predator *Paramecium tetraurelia*. Two of five experimental populations evolved multicellular structures not observed in unselected control populations within ~750 asexual generations. Considerable variation exists in the evolved multicellular life cycles, with both cell number and propagule size varying among isolates. Survival assays show that evolved multicellular traits provide effective protection against predation. These results support the hypothesis that selection imposed by predators may have played a role in some origins of multicellularity.

Nearly all macroscopic life is multicellular. As Leo Buss emphasized in *The Evolution of Individuality*, the very existence of integrated multicellular organisms is an outcome of evolutionary processes, not a starting condition[1]. It seems, in fact, to be a common outcome: multicellular organisms have evolved from unicellular ancestors dozens of times[2–4]. Animals, land plants, fungi, red algae, brown algae, several groups of green algae, cellular and acrasid slime molds, and colonial ciliates, among others, each descend from a different unicellular ancestor[4,5].

Two retrospective approaches, comparative methods and the fossil record, have proven valuable in reconstructing how these transitions may have occurred. Although both approaches have been critical to our understanding of early multicellular evolution, each has its limitations. For most multicellular groups, little or no fossil evidence exists that is relevant to the first steps in the transition from unicellular to multicellular life. Comparative methods suffer from a lack of intermediate forms between the multicellular organisms we are interested in and their extant unicellular relatives. Furthermore, direct knowledge of unicellular ancestors is not available. Extant unicellular relatives often serve as stand-ins, but this is a poor approximation, as they have been evolving independently as single-celled organisms since they diverged from their multicellular relatives.

A third, prospective, approach designed to circumvent these limitations has emerged in the last decade. The experimental evolution of multicellularity in otherwise unicellular microbes enables real-time observations of morphological, developmental, and genetic changes that attend the transition to multicellular life. Boraas and colleagues exposed cultures of the green alga *Chlorella vulgaris* to predation by the flagellate *Ochromonas vallescia*, resulting in the evolution of small, heritably stable algal colonies[6].

54 Becks and colleagues showed that exposure to the predatory rotifer *Brachionus calyciflorus*
55 selected for heritable changes in the rate of formation of multicellular palmelloids in the
56 green alga *Chlamydomonas reinhardtii*[7]. Ratcliff and colleagues have shown that selection
57 for an increased rate of settling out of liquid suspension consistently results in the evolution
58 of multicellular 'snowflake' colonies in the yeast *Saccharomyces cerevisiae*[8] and also
59 results in the evolution of simple multicellular structures in *C. reinhardtii*[9].

60 Predation has long been hypothesized as a cause for the evolution of
61 multicellularity, as most predators can only consume prey within a narrow range of
62 sizes[2,10–12]. Filter-feeding predators are common in aquatic ecosystems, and algae that are
63 larger than a threshold size are largely immune to them[10]. Thus, predation is an ecologically
64 plausible selective pressure that could explain at least some origins of multicellularity.

65 In this study, we present experiments in which we used the ciliate predator
66 *Paramecium tetraurelia* to select for the *de novo* evolution of multicellularity in outcrossed
67 populations of *C. reinhardtii*. We describe the heritable multicellular life cycles that
68 evolved and compare them to the ancestral, unicellular life cycle. In addition, we show that
69 the evolved multicellular life cycles are stable over thousands of asexual generations in the
70 absence of predators. Comparative assays show that the evolved multicellular phenotypes
71 provide a fitness advantage over its unicellular ancestor in the presence of predators.
72 Because *C. reinhardtii* has no multicellular ancestors, these experiments represent a
73 completely novel origin of obligate multicellularity[13,14].

74 **Results**

75 After 50 weekly transfers (~750 generations), simple multicellular structures evolved in
76 two of five predator-selected populations (B2 and B5). Such multicellular structures were
77 not observed in any of the control populations. Eight strains were isolated from each of
78 three populations (B2, B5, K1). We focused our analyses on five focal strains from B2 (B2-
79 01, B2-03, B2-04, B2-10, B2-11) and two strains from B5 (B5-05, B5-06). Of the isolates
80 from the control population that evolved in the absence of predators (K1), we analyzed two
81 strains (K1-01, K1-06). Phenotypes of other isolates from populations B2, B5 and K1 did
82 not differ qualitatively from the focal strains and were not investigated further. The strains
83 have maintained their evolved characteristics of simple multicellularity in the absence of
84 predators for four years as unfrozen, in-use laboratory strains. Therefore, we are confident
85 that the phenotypic traits that we report below are stably heritable.

86 Some strains, notably those from population B5, commonly formed stereotypic
87 eight-celled clusters, with an apparent unicellular and tetrad life stage (Fig. 1B). Other
88 strains, notably those from population B2, appeared to form amorphous clusters of variable
89 cell number (Fig. 1A). Other phenotypic differences could be easily discerned by light
90 microscopy. For example, in Fig. 1, an external membrane is visible around both evolved
91 multicellular colonies, indicating that they formed clonally via repeated cell division within
92 the cluster, rather than via aggregation.

93

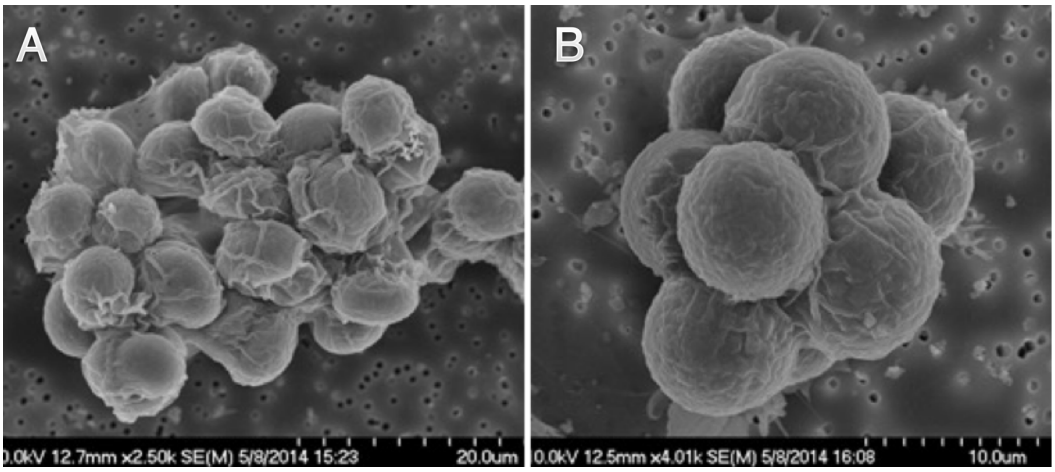

Figure 1. Scanning electron micrographs of representative multicellular colonies from evolved populations. [A] shows an amorphous cluster from population B2. Cell number varies greatly between clusters in this clone and between clones in this population. [B] shows an eight-celled cluster from population B5. Octads were frequently observed in both populations.

94 We found a variety of life cycles within and among populations. Using time-lapse
95 videos of evolved strains growing in liquid culture in 96-well tissue culture plates, we
96 qualitatively classified strains into four life cycle categories to compare their similarities
97 and differences (Fig. 2A-D). We discuss each life cycle category below, and then present
98 quantitative measurements on parent and propagule cluster sizes.

99

100

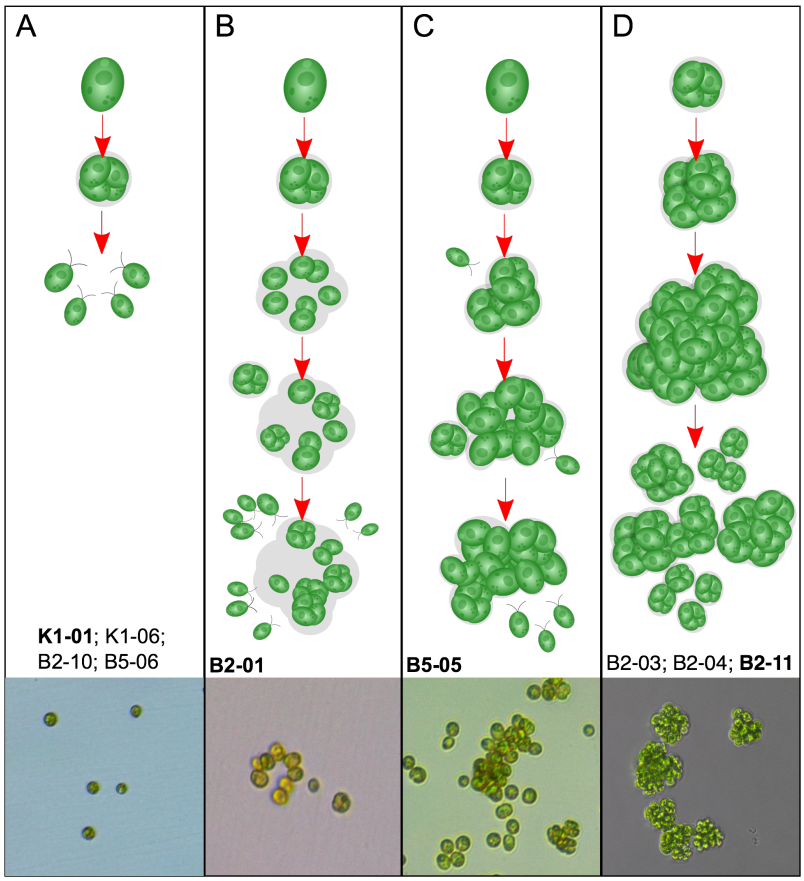

Figure 2. Depiction of *C. reinhardtii* life cycles following evolution with (B2, B5) or without (K1) predators for 50 weeks. Categories (A-D) show a variety of life cycle characteristics, from unicellular to various multicellular forms. Evolved strains were qualitatively categorized based on growth during 72-hour time-lapse videos. Strains within each life cycle category are listed below illustrations. Representative microscopic images of each life cycle category are at the bottom (Depicted strain in **boldface**).

101 In population K1, which evolved without predators, ancestral life cycle
102 characteristics of the unicellular, wild-type *C. reinhardtii* were retained (Fig. 2A,
103 Supplemental Videos 1 and 2). Specifically, as cells reproduce asexually, they lose motility
104 and undergo 2-5 rounds of mitosis before releasing motile, single-celled propagules. It
105 should be noted that even in wild-type *C reinhardtii*, the dividing parent cluster is a
106 *transient* multicellular stage; however, it does not persist after propagules are released.

107 Interestingly, in the two populations that evolved multicellularity in response to predation
108 (B2, B5), strains B5-06 and B2-10 retained a life cycle typical of the ancestral, wild-type
109 *C. reinhardtii* (Supplemental Videos 3 and 4, respectively).

110 Life cycles of the remaining strains isolated from populations B2 and B5 were
111 distinct from the ancestor, as clusters of various sizes persist through multiple rounds of
112 reproduction. Ordinarily, strain B2-01 releases motile, single-celled propagules during
113 reproduction, similar to the ancestor (Supplemental Video 5). However, in some clusters,
114 cells undergoing division separate, but remain proximately located because they are
115 embedded in an extracellular matrix (ECM) of the parent cluster (Fig. 2B). As these cells
116 continue to grow and divide, some remain embedded in the ECM, which creates growing
117 aggregations of cells. Strain B5-05 also produces motile, single-celled propagules that are
118 often embedded in the maternal ECM (Supplemental Video 6). In addition to retaining
119 propagules embedded in the ECM, growing clusters of B5-05 ensnare free-swimming cells,
120 creating aggregations that grow much larger than those of B2-01 (Fig. 2C).

121 Conversely, three of the strains isolated from population B2 exist in cell clusters
122 comprised only of direct descendants, as opposed to chimeric aggregations with free-
123 swimming cells. Clusters from strains B2-11, B2-03, and B2-04 grow in tightly associated
124 groups of direct descendants embedded in the maternal cell wall (Fig. 2D; Supplemental
125 Videos 7, 8, and 9, respectively). Development in these isolates is therefore strictly clonal,
126 with important implications for evolvability. Since the cells within a multicellular structure
127 are likely to be genetically identical, other than differences resulting from new mutations,
128 genetic variation in a population would be partitioned primarily among colonies. The clonal

129 development observed in these isolates therefore suggests that the observed multicellular
130 clusters would be well-suited to serving as units of selection.

131 In key respects, the isolates from population B2 appear to have recapitulated early
132 steps in volvocine evolution; in fact, the evolved multicellular algae are similar in their
133 gross morphology to small colonial volvocine algae such as *Pandorina*. Furthermore, a
134 degree of genetic control of cell number similar to that seen in undifferentiated colonial
135 volvocine algae manifests in our evolved multicellular strains. Propagules of these strains
136 are typically multicellular and, critically, no motile propagules were observed in these
137 strains. Propagules from the evolved multicellular strains were nearly all 4-, 8-, or 16-
138 celled, a range similar to that of small colonial volvocine algae and smaller than that of
139 *Pleodorina starrii,* in which propagules of a single genotype can span a 16-fold range of
140 cell numbers[15].

141 In order to determine the size attained by evolved strains, we sampled, stained, and
142 imaged growing cultures in tubes every 12 hours over a 6-day period. We find that cluster
143 sizes of strains that evolved without predators (K1-01, K1-06) and strains that retained
144 ancestral life cycle traits, despite evolving with predators (B5-06, B2-10), remain small
145 throughout the six days of growth (Fig. 3). Even at their largest, median cluster sizes of
146 replicate populations of strains K1-01 and K1-06 were all one cell per cluster, showing that
147 these strains exist as unicellular individuals with a transient a multicellular stage occurring
148 during reproduction. Similarly, we find that cells of strain B2-01 exist primarily as single
149 cells, with median sizes averaging 1.8 cells. Under time-lapse observation, we found that
150 dividing cells of B2-01 would occasionally separate from direct contact with each other
151 while still being held together by maternal ECM/cell wall. This was seen as white spaces

152 appearing between cells, which then remained equidistant in a rigid structure. During the
153 procedures to stain and image cells, it is possible that these semi-separated cells were
154 dispersed, leading to a slightly lower estimate of median cluster sizes. The median cluster
155 sizes of replicate populations of strain B5-05 averaged 4.0 cells, larger than strains that
156 retained the ancestral phenotype as well as B2-01. Unlike strains B2-01 and B5-05, in
157 which ECM holds cells in clusters, cells of the largest strains are visibly encapsulated
158 within the mother cell wall. Medians of replicate populations of these strains (B2-11, B2-
159 03, and B2-04) averaged 6.2, 5.6, and 5.6, respectively.

160 Because cells were mixed several times during the staining and imaging process, it
161 is possible that some clusters of cells were disrupted. Thus, cluster sizes from fluorescent
162 microscopy analysis are likely underestimates of cluster size, which may or may not affect
163 cluster size estimates for certain strains (i.e., those held together by extracellular matrix
164 rather than the maternal cell wall) more than others.

165

166

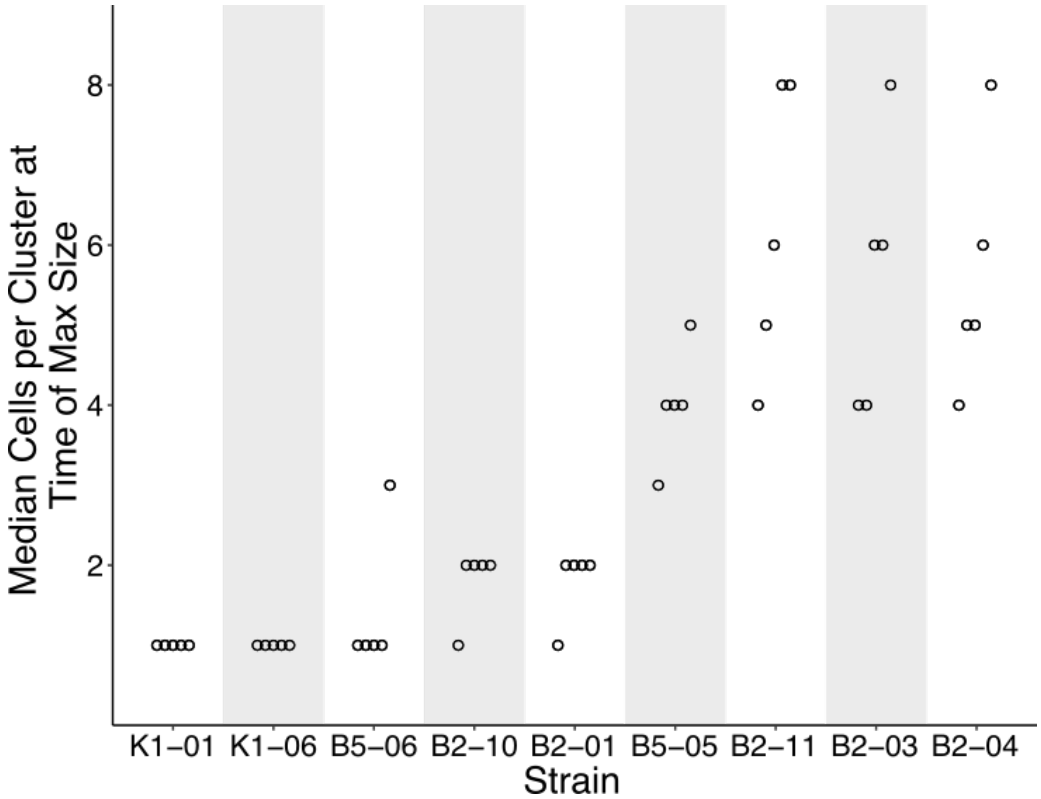

Figure 3. Median cluster sizes of evolved strains at the time-point where strains reached maximum size. To determine the time where strains were largest, we calculated the mean from five replicate medians (open dots), for each strain and time-point. Because data are not normally distributed, medians were chosen to approximate central tendency. Cells per cluster were measured by sampling strains over six days of growth, staining nuclei with DAPI, and imaging using fluorescent microscopy. From left to right, time-points of maximum size for each strain were: 12, 12, 72, 120, 96, 108, 84, 72, 72, 96, 96, and 72 hours. From left to right, median sizes of replicate populations averaged 1, 1, 1.4, 1.8, 1.8, 4, 6.2, 5.6, and 5.6 cells per cluster. Sizes at the initial time-point (0 hrs.) were omitted from analysis because they represent starting conditions. Shading is only for ease of visualization.

167

168 In order to determine propagule sizes of evolved strains, we manually analyzed 72-
169 hour time-lapse videos and recorded the numbers of cells in propagules released from
170 parent clusters. For most strains the majority of propagules were single-celled, as
171 observations were skewed toward smaller propagules, which require less biomass to

172 produce (Fig. 4). To accurately depict the context of individual cells in propagules, we also

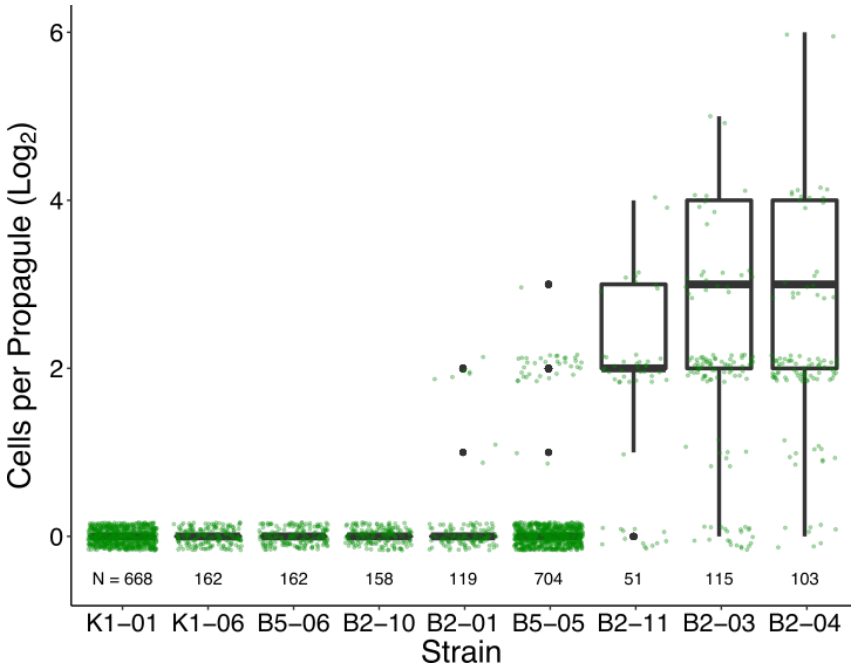

Figure 4. Sizes of propagules released by evolved strains during a 72-hour time-lapse. Propagule sizes were manually measured from time-lapse videos. Green dots show actual observations of propagule size. Because the frequency of observations is skewed toward smaller propagule sizes, we show the data as weighted boxplots as well, where a 32-celled propagule has 32 times the weight of a single-celled propagule. Sample sizes of propagule observations for each strain are indicated along the bottom of the plot. Strains are ordered by weighted-mean propagule size.

173 show the data as boxplots, weighted by biomass (Fig. 4, black boxplots). Strains that
174 maintained ancestral characteristics and had the smallest average maximum cluster sizes
175 (K1-01, K1-06, B5-06, B2-10) released almost exclusively single-celled propagules.
176 Although cells from strains B2-01 and B5-05 often exist in clusters, the vast majority of
177 propagules released by these reproducing clusters were single-celled as well. In strains with
178 larger average maximum cluster sizes (B2-11, B2-03, B2-04), cells are more frequently
179 released in multicellular propagules of up to 64 cells in size. Thus, among the strains that
180 evolved under predation, a variety of size-related traits emerged in both cluster size and
181 propagule size.

182

183 Multicellularity appears to provide an effective defense against predation.
184 Comparisons of predation rates were made by measuring the absorbance of each of the four
185 replicates without predators and dividing by the average of the four replicates with
186 predators. This value, labeled Δ_{abs}, shows markedly different trajectories for unicellular
187 and multicellular treatments with predators (Fig. 5). The unicellular strains, on average,
188 experienced ~2.5-fold greater rates of predation compared to the multicellular strains. That
189 is, the mean Δ_{abs} at hour 117 (day 5) were 0.367 and 0.140 for unicellular and multicellular
190 strains, respectively. To simplify the analysis, inferences were drawn from the final time-
191 point measurements (hour 117). A test for an effect of phenotype (unicellular or

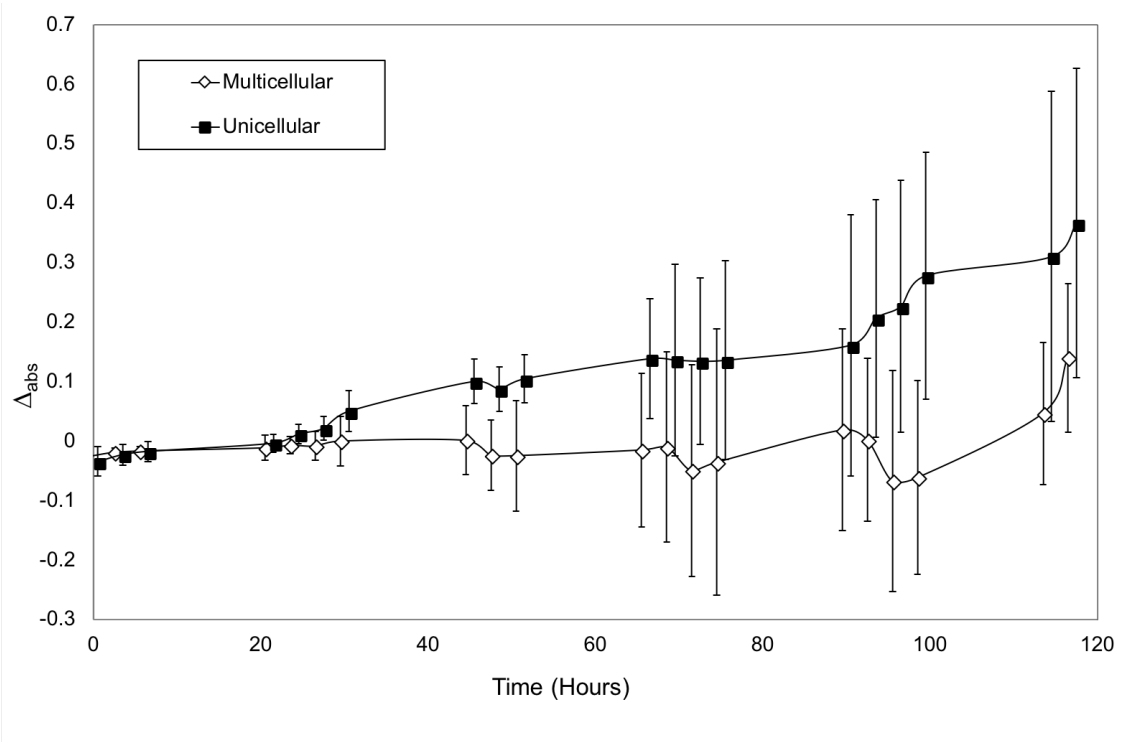

Figure 5. Average absorbance value differences (Δ_{abs}) between populations with and without predation for evolved multicellular and unicellular *C. reinhardtii* strains under predation. Multicellular strains averaged a much lower change in absorbance over the duration of the experiment than unicellular strains. Error bars are standard deviations of twelve strains per treatment. Markers are offset 0.5 h so that error bars can be seen.

192 multicellular) on Δ_{abs} values shows that phenotype has a strong effect on algal density
193 (ANOVA, $F_{1,22} = 8.65$, $P = 0.0076$).

194 **Discussion**

195 Our results show that the transition to a simple multicellular life cycle can happen rapidly
196 in response to an ecologically relevant selective pressure. By increasing in size beyond the
197 "predation threshold"[16] of a filter-feeding predator, multicellular *C. reinhardtii (*evolved
198 from an ancestrally unicellular lineage) are protected from predation for at least part of
199 their life cycle. Under selection for increased size, formation of multicellular structures
200 may be an easier route than increasing cell size because of trade-offs imposed by scaling
201 relationships (primarily the reduction in surface-area-to-volume ratio), because more
202 mutational paths are available, and/or because available mutations have fewer or less
203 severe pleiotropic effects.

204 These results support the view that predation may have played a role in at least
205 some origins of multicellularity. Consistent with previous results[6–9], predation can drive
206 the evolution of simple multicellular structures, and these structures provide protection
207 from predators[6,17]. The 'chicken-and-egg' problem brought up by some authors – that
208 multicellular predators are required to drive the evolution of multicellularity[e.g., 2,12] – does
209 not exist: unicellular filter-feeding protists exist, including, for example, *Paramecium*, and
210 there is no reason to think that such predators only arose after animals. Furthermore, some
211 origins of multicellularity, including those of brown and volvocine algae, postdate that of
212 animals, and could therefore have been driven by animal predation.

213

214 **Acknowledgments**

215 This work was supported by the National Science Foundation (DEB-1457701, DEB-
216 1456652), the John Templeton Foundation (43285), the NASA Astrobiology Institute
217 (NNA17BB05A), a NASA Postdoctoral Program Fellowship to MDH, and a Packard
218 Foundation Fellowship to WCR.

219

220 **Methods**

221 *Experimental evolution*

222 To increase genetic diversity at the onset of the experiment, we founded five experimental
223 (B1–B5) and three control (K1–K3) populations from an F1 cross. We obtained plus (CC-
224 1690) and minus (CC-2290) mating type strains of *C. reinhardtii* from the *Chlamydomonas*
225 Resource Center (www.chlamycollection.org) and crossed them using a protocol adapted
226 from Harris[18]. Vegetative cells were grown to high density in 10 mL TAP medium[19] at
227 22.5°C and pelleted in 15 mL conical tubes by centrifugation for 5 min. at 2000 × *g*.
228 Pelleted cells were resuspended in 10 mL mating medium (TAP minus NH_4Cl) and grown
229 in light for 6 h to induce gametogenesis. Gametes were mixed in a 24-well tissue culture
230 plate with 0.5 mL of each mating type, incubated in light for 4 h, and then dried in the dark.
231 Single mating-type controls of 1 mL were treated identically to ensure that no vegetative
232 material survived desiccation. After 20 days in the dark, crosses and single mating-type
233 controls were each flooded with 1 mL TAP medium and placed in light at 22.5°C to
234 germinate. Single mating-type controls showed no evidence of vegetative growth after two

235 weeks; thus, desiccation was effective in killing vegetative material and surviving algae
236 from the crosses must be outcrossed.

237 Experimental populations were started by mixing 0.1 mL of *C. reinhardtii* F1
238 cultures, grown to ~2×10^6 cells/mL, with 0.1 mL of a culture of *P. tetraurelia*, grown to
239 ~2×10^5 cells/mL, in 1.3 mL of COMBO medium[20], making a final volume of 1.5 mL.
240 Control populations were founded by inoculating 0.1 mL of *C. reinhardtii* F1 cultures in
241 1.4 mL of COMBO medium. All populations were propagated in 24-well plates and
242 transferred weekly.

243 During transfers, populations were homogenized with a multichannel pipette by
244 drawing and dispensing 1 mL three times. After mixing, 0.1 mL of culture was transferred
245 to 1.4 mL fresh COMBO in a new 24-well plate. After 350 days, populations were plated
246 on TAP medium + 1.5% agar. For each population plate, eight individual colonies were
247 randomly picked and re-plated on agar. Individual colonies were picked and re-plated at
248 least three times each to ensure that each was monoclonal and free of contaminants.

249 We initially characterized evolved phenotypes using light microscopy. A
250 homogenized dilution of each isolate grown in TAP medium was fixed in iodine and stored
251 at 4°C. For each isolate, 48 μL samples were photographed in replicate on a
252 hemocytometer. Images for each of the clones were processed in ImageJ to determine
253 particle counts and relative particle sizes, and these data were later processed in Python to
254 determine the relative proportions of different sized particles. The size threshold used to
255 distinguish between unicellular and multicellular particles was user-determined and was
256 rarely violated by any samples. In all instances where the size threshold was violated, small
257 multicellular particles were categorized as unicellular; thus, we remain conservative in our

258 characterization of particle sizes, under- rather than overestimating the number of cells in
259 particles.
260
261 *Maximum Cells Per Cluster*
262 In order to determine the size attained by different evolved strains, measured as the
263 maximum number of cells per cluster, we stained and imaged samples via fluorescent
264 microscopy over a 6-day examination period. Strains were cultured in 10 mL of TAP
265 medium in a climate-controlled chamber on a 14:10-hour light:dark cycle (23.5ºC, 41%
266 humidity, 326 lx). In order to standardize starting cell concentrations, preliminary cultures
267 were first inoculated from scrapes of colonies on TAP plates (2% agar) and allowed to
268 grow, without disruption, for 6 days until reaching stationary phase. Cultures were then
269 transferred 1:100 into fresh TAP medium and examined over the following 6-day
270 examination period.
271 Throughout the examination period, cultures were sampled, stained, and imaged
272 every 12 hours in order to capture the maximum size attained by various strains before
273 reaching stationary phase. Strains B5-05 and B5-06 were not sampled at the final time-
274 point. Samples were extracted from well-mixed culture tubes and transferred into 1.5 mL
275 microcentrifuge tubes (200 μL from the first 6 time-points to compensate for low cell
276 density, 100 μL from all time-points thereafter). The samples were centrifuged at 250 x *g*
277 for 5 minutes and the supernatant was replaced by a 50% v/v ethanol-water solution to fix
278 cells and make cell membranes more permeable to the DAPI (4',6-diamidino-2-
279 phenylindole) fluorescent nucleotide stain. After a 10-minute fixation period, samples were
280 centrifuged again (250 x *g* for 5 minutes) and the supernatant was replaced with distilled

281 water containing 1 μg/mL DAPI. Cells with DAPI were kept in darkness for one hour and
282 then moved to a refrigerator without light to prevent photo bleaching until imaging on the
283 microscope.

284 Prior to imaging, samples were removed from the refrigerator and inverted to mix
285 cultures. Seven μL of each sample were mounted on glass microscope slides and large 6 ×
286 6 images were stitched from individual images captured at 40x magnification, creating
287 high-resolution (441 megapixel) wide-field images, providing a robust measurement of the
288 distribution of clusters sizes within the population.

289

290 *Image and data analysis*

291 Large stitched images of individual samples were imported and analyzed in Fiji[21]. We
292 wrote and implemented a script in ImageJ macro (Supplemental Material) to automatically
293 calculate the number of cells in each cluster. The script accomplished this by demarcating
294 cluster boundaries and recording the number of pixel maxima within each boundary,
295 corresponding to the number of DAPI-stained nuclei. Following this procedure, all images
296 used in our analyses were manually screened and any regions of interest resulting from
297 artifacts (*e.g.,* dust particles, autofluorescence) were removed from the dataset. Data for
298 five technical replicates of all tested strains, each represented by 12 time-points sampled
299 over six days, were concatenated into one large dataset.

300 In order to determine the maximum number of cells per cluster achieved by each
301 strain, hereafter referred to as "cluster size", we first determined the time-point at which
302 clusters were largest. This was calculated separately for each strain, as different strains
303 reached their maximum size at different time-points during the six-day culture cycle. First,

304 we calculated the median cluster size of each replicate at each time-point throughout the
305 culture cycle. Medians were chosen to represent the central tendency instead of the mean
306 because the distributions of cluster sizes were right-skewed and occasionally contained
307 large outlier clusters. Then, to determine the time-point at which cluster size was largest
308 for each strain, we calculated the average (mean) of the median cluster sizes from replicate
309 populations within each time-point. The first time-point, representing cluster sizes at time
310 of inoculation, was removed from analysis.

311

312 *Number of Cells per Propagule*

313 In order to determine the number of cells per propagule released by clusters of each strain,
314 hereafter referred to as "propagule size", we time-lapse imaged all strains over 72 hours of
315 growth. First, cells were inoculated from colonies on TAP agar plates into liquid TAP
316 media and incubated for five days to grow to high density. Then, each culture was
317 homogenized by vortexing, transferred 1:100 into five replicate tubes of fresh TAP media,
318 and allowed to grow for two days. These exponentially growing cultures were mixed by
319 vortexing, diluted 1:10 in TAP medium, and then 100 μL from each culture was randomly
320 inoculated into the central 60 wells of a 96-well tissue culture plate that already contained
321 100 μL of TAP medium in each well.

322 For time-lapse microscopy, the 96-well plate (containing five technical replicates
323 of each strain) was imaged at 200x magnification, where the field of view was positioned
324 on cells near the center and at the bottom of wells. The time-lapse was run for 72 hours,
325 capturing images of each well every 30 minutes.

326 Time-lapse images were manually analyzed using ImageJ. For each well, all images
327 from the time-lapse were viewed individually and sequentially. All cells or clusters of cells
328 in the frame at the beginning of the time-lapse were labeled with a number indicating their
329 identity. Throughout the time-lapse, when a cell or cluster of cells was seen to separate
330 from the initial parental cluster/group, the number of cells in the propagule was recorded.
331 For wells that had few or no initial cells in the frame (typically occurring for motile,
332 unicellular strains), cells or clusters of cells were labeled as they entered the field of view,
333 until collecting a sufficient sample size (N > 5 parental clusters). Due to the long time
334 required for clusters to fully separate physically—even after they have detached from a
335 parent cluster—propagule sizes were recorded four frames (two hours) after the propagule
336 was observed to initially split from the parental cluster. Data collected from time-lapse
337 images were analyzed in R[22].
338
339 *Defense against predators*
340 To test whether multicellularity affords protection from predators, we subjected evolved
341 unicellular and multicellular isolates to predation by the rotifer *Brachionus calyciflorus*.
342 Rotifers were chosen for this assay instead of *Paramecium* to reduce the likelihood that
343 some adaptation other than cluster formation protected cluster-forming strains from the
344 predator. Rotifers were obtained as cysts in vials and stored at 4°C in the dark. To ensure
345 that cultures of *B. calyciflorus* were free of contaminants, cysts were treated and incubated
346 according to the protocol described by Suga *et al.*[23]. Neonate rotifers were grown
347 axenically in 10 mL of WC medium[24] with 100 µg/mL ampicillin in culture tubes at the
348 same temperature and light conditions as the *C. reinhardtii* cultures. In order to sustain the

349 population of *B. calyciflorus* before the experiment, 1.0 mL of an axenic, unicellular strain
350 of *C. reinhardtii*, CC-1690, was inoculated into the culture via micropipette.

351 Evolved isolates of *C. reinhardtii* were grown to high density, and culture
352 absorbance was measured using a microplate reader (Molecular Devices SpectraMax®
353 M5, 420 nm), whereafter each was diluted to approximately 3.45×10^5 cells/mL. Four
354 replicates of each strain were randomly assigned to 24-well plates and 1.33 mL of each
355 strain pipetted into designated wells. Twelve multicellular strains (B2-03, 04, 06, 07, and
356 11; B5-01 through 07) and twelve unicellular strains (B2-01, 10, and 12; B5-08; K1-01,
357 02, and 04 through 09) were used for this assay. Rotifer cultures were poured through a 25
358 μm mesh filter to remove the algae they had been feeding on, then pipetted into a sterile
359 test tube awaiting transfer to the experimental wells (*C. reinhardtii* cells are ~10 μm in
360 diameter and easily pass through the filter). Depending on the treatment condition, 0.67
361 mL of either WC medium or WC medium with predators was added to each well. Initial
362 absorbance values were recorded and then plates were stored under lights in an incubator
363 on a 14/10-hour light/dark cycle at 22.5 °C for 5 days. Throughout the 14-hour light period,
364 absorbance readings were taken every 3 hours, providing growth rates with high resolution
365 for all strains.

366

367 **References**

368 1. Buss, L. W. *The Evolution of Individuality*. (Princeton University Press, 1987).
369 2. Bonner, J. T. The origins of multicellularity. *Integr. Biol.* **1,** 27–36 (1998).
370 3. Kaiser, D. Building a multicellular organism. *Annu. Rev. Genet.* **35,** 103–23
371 (2001).

372 4. Grosberg, R. K. & Strathmann, R. R. The evolution of multicellularity: a minor
373 major transition? *Annu. Rev. Ecol. Evol. Syst.* **38,** 621–654 (2007).
374 5. Herron, M. D., Rashidi, A., Shelton, D. E. & Driscoll, W. W. Cellular
375 differentiation and individuality in the 'minor' multicellular taxa. *Biol. Rev. Camb.*
376 *Philos. Soc.* **88,** 844–861 (2013).
377 6. Boraas, M. E., Seale, D. B. & Boxhorn, J. E. Phagotrophy by a flagellate selects
378 for colonial prey: a possible origin of multicellularity. *Evol. Ecol.* **12,** 153–164
379 (1998).
380 7. Becks, L., Ellner, S. P., Jones, L. E. & Hairston, N. G. Reduction of adaptive
381 genetic diversity radically alters eco-evolutionary community dynamics. *Ecol.*
382 *Lett.* **13,** 989–997 (2010).
383 8. Ratcliff, W. C., Denison, R. F., Borrello, M. & Travisano, M. Experimental
384 evolution of multicellularity. *Proc. Natl. Acad. Sci. USA* **109,** 1595–1600 (2012).
385 9. Ratcliff, W. C. *et al.* Experimental evolution of an alternating uni- and
386 multicellular life cycle in Chlamydomonas reinhardtii. *Nat. Commun.* **4,** 2742
387 (2013).
388 10. Bell, G. *The origin and early evolution of germ cells as illustrated by the*
389 *Volvocales*. *The Origin and Evolution of Sex* (Alan R. Liss, 1985).
390 11. Stanley, S. M. An ecological theory for the sudden origin of multicellular life in
391 the Late Precambrian. *Proc. Natl. Acad. Sci. USA* **70,** 1486–1489 (1973).
392 12. Pentz, J. T., Limberg, T., Beermann, N. & Ratcliff, W. C. Predator escape: an
393 ecologically realistic scenario for the evolutionary origins of multicellularity. *Evol.*
394 *Educ. Outreach* **8,** 13 (2015).

395 13. Herron, M. D. & Michod, R. E. Evolution of complexity in the volvocine algae:
396 Transitions in individuality through Darwin's eye. *Evolution* **62,** 436–451 (2008).
397 14. Leliaert, F. *et al.* Phylogeny and molecular evolution of the green algae. *CRC.*
398 *Crit. Rev. Plant Sci.* **31,** 1–46 (2012).
399 15. Herron, M. D., Ghimire, S., Vinikoor, C. R. & Michod, R. E. Fitness trade-offs
400 and developmental constraints in the evolution of soma: An experimental study in
401 a volvocine alga. *Evol. Ecol. Res.* **16,** 203–221 (2014).
402 16. Kirk, D. L. *Volvox: Molecular-Genetic Origins of Multicellularity*. (Cambridge
403 University Press, 1998).
404 17. Becks, L., Ellner, S. P., Jones, L. E. & Hairston, N. G. The functional genomics of
405 an eco-evolutionary feedback loop: linking gene expression, trait evolution, and
406 community dynamics. *Ecol. Lett.* **15,** 492–501 (2012).
407 18. Harris, E. H. *The Chlamydomonas Sourcebook, Second Edition*. (Academic Press,
408 2009).
409 19. Gorman, D. S. & Levine, R. P. Cytochrome F and plastocyanin: their sequence in
410 the photosynthetic electron transport chain of Chlamydomonas reinhardtii. *Proc.*
411 *Natl. Acad. Sci. USA* **54,** 1665–1669 (1965).
412 20. Kilham, S. S., Kreeger, D. A., Lynn, S. G., Goulden, C. E. & Herrera, L. COMBO:
413 A defined freshwater culture medium for algae and zooplankton. *Hydrobiologia*
414 **377,** 147–159 (1998).
415 21. Schindelin, J. *et al.* Fiji: an open-source platform for biological-image analysis.
416 *Nat. Methods* **9,** 676–682 (2012).
417 22. R Development Core Team. R: A Language and Environment for Statistical

Computing. (2009).

23. Suga, K., Tanaka, Y., Sakakura, Y. & Hagiwara, A. Axenic culture of Brachionus plicatilis using antibiotics. *Hydrobiologia* **662,** 113–119 (2011).

24. Guillard, R. R. L. in *Culture of Marine Invertebrate Animals* (eds. Smith, W. L. & Chantey, M. H.) 29–60 (Plenum Publishers, 1975).

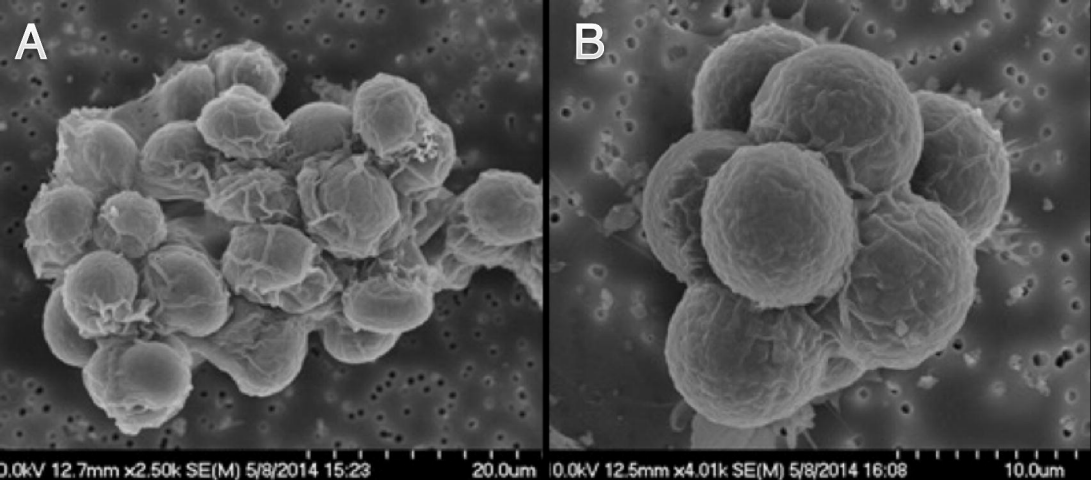
A
B
0.0kV 12.7mm x2.50k SE(M) 5/8/2014 15:23
20.0um
0.0kV 12.5mm x4.01k SE(M) 5/8/2014 16:08
10.0um

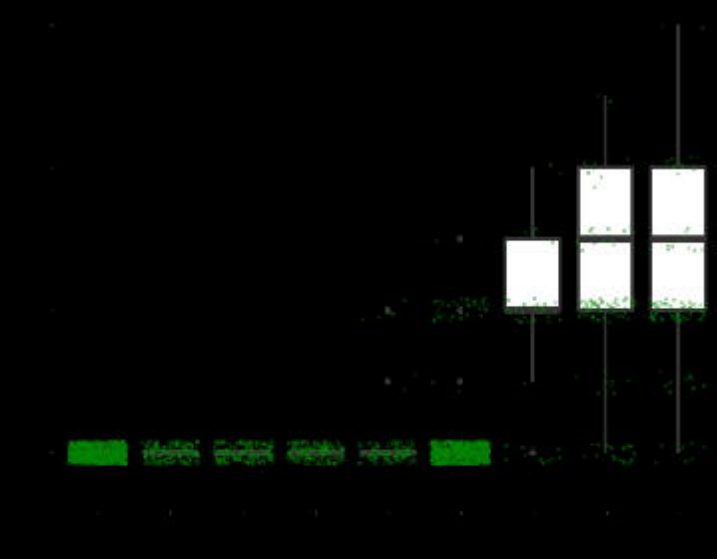

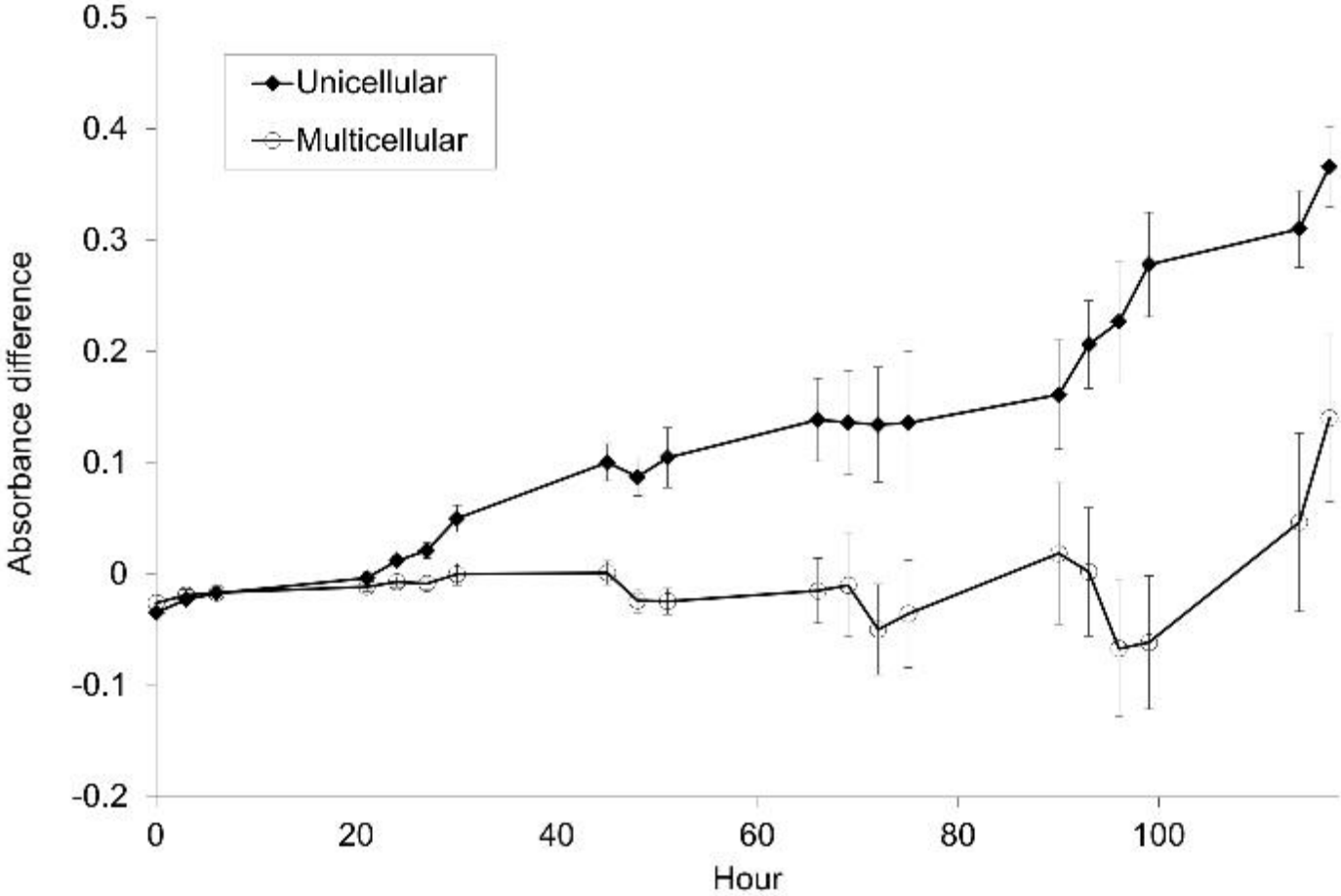
Unicellular
Multicellular
Absorbance difference
Hour
0.5
0.4
0.3
0.2
0.1
0
-0.1
-0.2
0
20
40
60
80
100